


Lindblad quantum dynamics from correlation functions of classical spin chains

Markus Kraft ^{1,*} Mariel Kempa ¹ Jiaozi Wang ¹ and Robin Steinigeweg ^{1,†}

¹*University of Osnabrück, Department of Mathematics/Computer Science/Physics, D-49076 Osnabrück, Germany*

(Dated: January 28, 2025)

The Lindblad quantum master equation is one of the central approaches to the physics of open quantum systems. In particular, boundary driving enables the study of transport, where a steady state emerges in the long-time limit, which features a constant current and a characteristic density profile. While the Lindblad equation complements other approaches to transport in closed quantum systems, it has become clear that a connection between closed and open systems exists in certain cases. Here, we build on this connection for magnetization transport in the spin-1/2 XXZ chain with and without integrability-breaking perturbations. Specifically, we study the question whether the time evolution of the open quantum system can be described on the basis of classical correlation functions, as generated by the Hamiltonian equations of motion for real vectors. By comparing to exact numerical simulations of the Lindblad equation, we find a good accuracy of such a description for a range of model parameters, which is consistent with previous studies on closed systems. While this agreement is an interesting physical observation, it also suggests that classical mechanics can be used to solve the Lindblad equation for comparatively large system sizes, which lie outside the possibilities of a quantum mechanical treatment. We also point out counterexamples and limitations for the quantitative extraction of transport coefficients. Remarkably, our classical approach to large open systems allows to detect superdiffusion at the isotropic point.

I. INTRODUCTION

Many-body quantum systems out of equilibrium can be studied in two complementary scenarios. Either, the system is closed and couples by no means to the rest of the world. Or, the system is open and explicitly couples to a bath, where the system-bath coupling can be weak or strong. Both scenarios are interesting and important by their own right and allow to address a large variety of questions in modern physics, ranging from fundamental questions in statistical mechanics to applied questions in material science. A central question in closed and open scenarios is the system's evolution in the course of time and the existence and properties of steady states in the long-time limit [1–5]. The study of this particular question has seen remarkable progress in the past, due to experimental advances [6], fresh theoretical concepts like typicality of pure quantum states [7–15] and eigenstate thermalization [16–18], and the development of sophisticated numerical techniques [19, 20].

Within the diverse class of nonequilibrium processes, transport is a natural one for systems with one or more globally conserved quantities [21], like total energy, particle number, or magnetization. Transport is further a process which is relevant to both, closed and open situations. In an open situation, the system of actual interest can be coupled at its boundaries to two reservoirs at different temperatures or chemical potentials, such that transport is induced and a nonequilibrium steady state is usually established in the long-time limit [22–24]. In this steady state, the constant current and the form of the density profile yield information on the qualitative

type of transport and also allow to determine quantitative values for transport coefficients [21]. A widely used strategy to describe such an open scenario is the Lindblad equation [25], which has its assets and drawbacks. On the one hand, the derivation of this equation from a microscopic system-bath model can be a nontrivial task in praxis [26, 27]. On the other hand, it is the most general form of a quantum master equation, which Markovian and maps any density matrix to a density matrix again. Furthermore, the structure of the Lindblad equation enables the application of well-suited numerical techniques. Here, one method is provided by the concept of stochastic unraveling [28, 29], which constructs the time evolution of the density matrix in Liouville space as the average over many pure-state trajectories in Hilbert space. An alternative method is given by matrix product states [23, 30–32], where entanglement growth is reduced because of dissipation.

In closed systems, a main approach is linear response theory, which predicts the behavior close to equilibrium in terms of correlation functions at equilibrium. While in the context of transport the current autocorrelation is a central object and enters the well-known Kubo formula [33], the transport behavior is also encoded in density-density correlations, which can be analyzed in real or momentum space and in the time or frequency domain. Even though the investigation of correlation functions has a long and fertile history, the concrete calculation for specific models can still be a challenging task in praxis. In particular, seemingly simple models like the integrable spin-1/2 XXZ chain have turned out to be notoriously difficult for both, analytical and numerical methods [21]. Models of interacting spins are valuable, because they are not only many-body quantum systems with rich phase diagrams, but also have a classical counterpart [34–61], which corresponds to the limit of large spin quantum

* markus.kraft@uos.de

† rsteinig@uos.de

numbers $S \rightarrow \infty$. While the cases of $S = 1/2$ and $S \rightarrow \infty$ can in general not be expected to exhibit the same physics, it has been observed that their dynamics is similar for some examples [62, 63], qualitatively and also quantitatively. Such a similarity has been found for correlation functions in the XXZ chain in the limit of high temperatures $T \rightarrow \infty$ [64, 65], where the low-energy excitations are less relevant [66].

In this paper, we also investigate to what extent the time evolution in a quantum system can be described on the basis of the dynamics in the classical counterpart. In contrast to previous works, which have been devoted to a comparison of the corresponding correlation functions in a closed scenario [64, 65], we intend to go a substantial step beyond. Specifically, we are going to compare the open quantum system to the closed classical system. For such a comparison, we obviously need a connection between the dynamics in open and closed scenarios [67, 68], which does not exist in general [69–71]. For the spin-1/2 chain, however, a connection has been recently suggested [72] for the case of small system-bath coupling and weak driving. Because this connection involves quantum correlation functions, we replace them by the corresponding classical ones. In this way, we can address the main question of our work: Is it possible to obtain Lindblad quantum dynamics from correlation functions of classical spin chains? To answer this question, we compare to exact numerical simulations of the Lindblad equation. We observe a good agreement for a range of model parameters, which is consistent with previous studies on closed systems. This agreement further hints that classical mechanics can be used as a strategy to solve the Lindblad equation for large system sizes, which are not accessible in a quantum mechanical treatment. Such a classical strategy has been also discussed in other open quantum systems [73]. We also point out counterexamples and limitations for the quantitative extraction of transport coefficients. Remarkably, our classical approach to large open systems allows to detect superdiffusion at the isotropic point.

This paper is structured as follows: We introduce the open quantum system in Sec. II. Then, we discuss the connection between open and closed systems in Sec. III and the classical limit in Sec. IV. Next, we present our numerical results in Sec. V. We close with a summary and conclusion in Sec. VI. Further information can be found in the appendix.

II. OPEN QUANTUM SYSTEM

Let us start by introducing the open quantum system considered throughout this work. We choose to describe this system by the Lindblad equation,

$$\dot{\rho}(t) = \mathcal{L}\rho(t) = i[\rho(t), H] + \mathcal{D}\rho(t), \quad (1)$$

as the most general form of a quantum master equation, which is Markovian and maps any density matrix to a

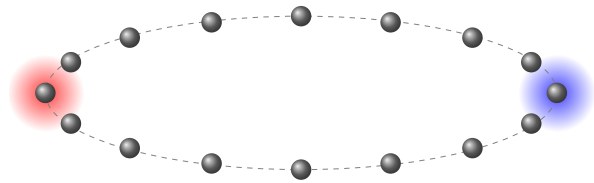


FIG. 1. Geometry of the open quantum system. The spin-1/2 XXZ chain with periodic boundary conditions is coupled to two Lindblad baths, which are located at a site $B_1 = 1$ and another site $B_2 = N/2 + 1$.

density matrix again [25]. While the first term on the r.h.s. is coherent and describes the unitary time evolution w.r.t. to a given Hamiltonian H , the second term on the r.h.s. is incoherent and describes the damping due to the presence of a bath. This damping reads

$$\mathcal{D}\rho(t) = \sum_j \alpha_j \left(L_j \rho(t) L_j^\dagger - \frac{1}{2} \{ \rho(t), L_j^\dagger L_j \} \right) \quad (2)$$

with Lindblad operators L_j , non-negative rates α_j , and the anticommutator $\{\bullet, \bullet\}$.

Next, we define the Hamiltonian H and a suitable set of Lindblad operators L_j . Focusing first on H , we choose the spin-1/2 XXZ chain [21],

$$H = J \sum_{r=1}^N (S_r^x S_{r+1}^x + S_r^y S_{r+1}^y + \Delta S_r^z S_{r+1}^z), \quad (3)$$

where S_r^j ($j = x, y, z$) are the components of a spin-1/2 operator at site r , N is the number of sites, $J > 0$ is the antiferromagnetic coupling constant, and Δ is the anisotropy in z direction. We assume periodic boundary conditions, $S_{N+1}^j = S_1^j$, which are for our purposes more convenient than open boundary conditions, as discussed later.

Because the Hamiltonian in Eq. (3) is integrable for all possible values of the anisotropy Δ , we additionally take into account an integrability-breaking perturbation. Our choice for such a perturbation are interactions between next-to-nearest sites,

$$H' = H + \Delta' \sum_{r=1}^N S_r^z S_{r+2}^z, \quad (4)$$

where Δ' is the perturbation strength and, as before, we assume periodic boundary conditions.

For each of the Hamiltonians in Eqs. (3) and (4), the total magnetization $S^z = \sum_r S_r^z$ is a strictly conserved quantity, $[H, S^z] = [H', S^z] = 0$. Thus, the transport of local magnetization is a meaningful question. The study of transport also motivates our choice of the Lindblad operators L_j . Specifically, we make a simple but common

choice [21],

$$L_1 = S_{B_1}^+, \quad \alpha_1 = \gamma(1 + \mu), \quad (5)$$

$$L_2 = L_1^\dagger = S_{B_1}^-, \quad \alpha_2 = \gamma(1 - \mu), \quad (6)$$

$$L_3 = S_{B_2}^+, \quad \alpha_3 = \gamma(1 - \mu), \quad (7)$$

$$L_4 = L_3^\dagger = S_{B_2}^-, \quad \alpha_4 = \gamma(1 + \mu), \quad (8)$$

where γ is the system-bath coupling and μ is the driving strength. The local operators L_1 and L_2 act on the site B_1 and flip a spin up and down, respectively. The other operators L_3 and L_4 act in the same way on another site B_2 . To maximize the size of the bulk, we set $B_1 = 1$ and $B_2 = N/2 + 1$, as illustrated in Fig. 1. Due to the choice of the rates in Eqs. (5) - (8), net magnetization flows from the first bath into the system and from the system into the second bath, which leads to a nonequilibrium steady state in the long-time limit.

For this open quantum system, we are interested in the dynamics of local magnetization, which includes the steady-state profile on the one hand and its buildup in time on the other hand. Hence, we study the expectation value

$$\langle S_r^z(t) \rangle = \text{tr}[S_r^z \rho(t)], \quad (9)$$

which depends on the Hamiltonian H , but also on the system-bath coupling γ and the driving strength μ . We focus on the case of small γ and μ . As initial condition, we use the ensemble

$$\rho(0) = \frac{e^{-\beta H}}{\text{tr}[e^{-\beta H}]} \quad (10)$$

for high temperatures $\beta = 1/T \rightarrow 0$, which features a homogeneous profile of magnetization.

An exact analytical solution of the Lindblad equation, or an accurate approximation of it, can in general not be derived. Hence, one has to resort typically to numerical methods. In this context, standard exact diagonalization is particularly challenging [74], since the Liouville space (of dimension $D = 2^N \times 2^N$) is substantially larger than the anyhow large Hilbert space ($D = 2^N$). Yet, the Lindblad form allows for stochastic unraveling [28, 29], which yields the time-dependent density matrix as the average over many pure-state trajectories. Additionally, simulations on the basis of matrix product states [23, 30–32] give access to systems of hundreds of spins, at least on time scales with a still low amount of entanglement.

In this work, we mostly rely on existing numerical data in the literature [72, 75], which we use later for a comparison to our approach on the basis of classical mechanics. Before we explain what we mean by classical mechanics, we need to discuss another concept, i.e., a connection between the dynamics in open and closed quantum systems.

III. CONNECTION BETWEEN OPEN AND CLOSED SYSTEMS

In general, one can hardly expect a direct connection between the time evolution in open and closed quantum systems. For the specific scenario introduced in Sec. II, however, such a connection has been shown to exist, at least in certain cases [72]. This connection makes use of spatio-temporal correlation functions,

$$\langle S_r^z(t) S_{r'}^z(0) \rangle_{\text{eq}} = \frac{\text{tr}[e^{-\beta H} e^{iHt} S_r^z e^{-iHt} S_{r'}^z]}{\text{tr}[e^{-\beta H}]}, \quad (11)$$

which are evaluated in the closed system H at thermal equilibrium. For high temperatures $\beta = 1/T \rightarrow 0$, which we use from now on, they simplify to

$$\langle S_r^z(t) S_{r'}^z(0) \rangle_{\text{eq}} = \frac{\text{tr}[e^{iHt} S_r^z e^{-iHt} S_{r'}^z]}{2^N}. \quad (12)$$

Before we formulate the actual connection, it is useful to introduce a superposition of Eq. (12) with $r' = B_1$ and Eq. (12) with $r' = B_2$,

$$C_r(t) = \langle S_r^z(t) S_{B_1}^z(0) \rangle_{\text{eq}} - \langle S_r^z(t) S_{B_2}^z(0) \rangle_{\text{eq}}, \quad (13)$$

and then to define the more complex superposition

$$d_r(t) = 2\mu \sum_j A_j \Theta(t - \tau_j) C_r(t - \tau_j), \quad (14)$$

where A_j are some amplitudes, τ_j are some times, and $\Theta(t)$ is the Heavyside function. Using this notation, we can eventually formulate the connection and express the nonequilibrium dynamics of the open system in Eq. (9) as [72]

$$\langle S_r^z(t) \rangle \approx \frac{1}{T_{\text{max}}} \sum_{T=1}^{T_{\text{max}}} d_{r,T}(t), \quad (15)$$

where the sum runs over T_{max} different time sequences (τ_1, τ_2, \dots) . This sum over time sequences gives rise to the additional index T , which is absent in Eq. (14). Here, a particular time sequence is generated by

$$\tau_{j+1} = \tau_j - \ln \frac{\varepsilon_{j+1}}{2\gamma}, \quad (16)$$

where ε_{j+1} are random numbers drawn from a uniform distribution in the interval $]0, 1]$. The amplitudes A_j , as derived in [72], are now given by

$$A_j = \frac{a_j - d_{B_1,T}(\tau_j - 0^+)}{\mu} \quad (17)$$

with

$$a_j = \frac{\mu - 2 d_{B_1,T}(\tau_j - 0^+)}{2 - 4\mu d_{B_1,T}(\tau_j - 0^+)}. \quad (18)$$

These amplitudes follow from $d_{B_1,T}(\tau_j - 0^+)$, which is evaluated at the bath-contact site B_1 and just before the

time τ_j . Therefore, A_j only depends on A_{j-1}, \dots, A_1 . If $d_{B_1}(\tau_j - 0^+) \rightarrow 0$, $A_j \rightarrow 1/2$. Note that $A_1 = 1/2$ by construction. Loosely speaking, A_j can be understood as the current “boundary condition” of the density profile, which should not be confused with the actual boundary condition of the Hamiltonian.

While the connection might look quite complicated at first sight, it is rather simple, especially since it expresses the nonequilibrium dynamics in the open system just as a superposition of equilibrium correlation functions in the closed system. As discussed in Ref. [72] in detail, such a connection cannot always hold and requires sufficiently small values of both, γ and μ . Thus, one has to check in practise that the result for a given model and a specific choice of the parameters γ and μ does not change when these parameters get smaller and smaller.

A sophisticated criterion for the smallness of the two parameters also exists and has been studied in Ref. [75] in detail. Loosely speaking, the life time of an excitation, which is injected at the boundary of the model, has to be short compared to the time scale $1/\gamma$. More formally, the autocorrelation function at the bath-contact site,

$$\langle S_{B_1}^z(t) S_{B_1}^z(0) \rangle_{\text{eq}} \quad (19)$$

has to decay on this time scale. For the specific case of periodic boundary conditions, which are used throughout our work, this condition can be satisfied by a sufficiently small γ and hence long enough $1/\gamma$. For the other case of open boundary conditions, however, the autocorrelation function does not decay at all for $\Delta > 1$, see Ref. [75] and also Refs. [76, 77].

To understand the sophisticated criterion for μ , one has to resort to stochastic unraveling, which underlies the derivation of the connection in Eq. (15) [72]. In this context, μ has then to be negligible for the deterministic evolution up to the average jump time $1/\gamma$. For the jump probabilities, however, μ is fully taken into account and gives rise to the amplitudes in Eq. (17). Alternatively, by taking a more physical point of view, the smallness of μ might be seen as a requirement of linear response theory, which then naturally leads to the correlation functions in the connection (15). More details on the validity range and physical meaning can be found in Refs. [72, 75].

In Fig. 2, we illustrate the quality of the connection, by comparing the prediction on the r.h.s. of Eq. (15) to a simulation based on stochastic unraveling for the l.h.s. of Eq. (15). We do so for the model H' in Eq. (4) with $\Delta = 1.5$, $\Delta' = 0$, $N = 20$, periodic boundary conditions, small coupling $\gamma/J = 0.1$, and weak driving $\mu = 0.1$. For this set of parameters, the agreement between both sides is remarkable. (Note that stochastic unraveling as such neither requires small γ nor weak μ .) While Fig. 2 shows existing data from the literature [72], it already depicts a prediction by the use of classical mechanics, as a main result of our work. This prediction is discussed in the following.

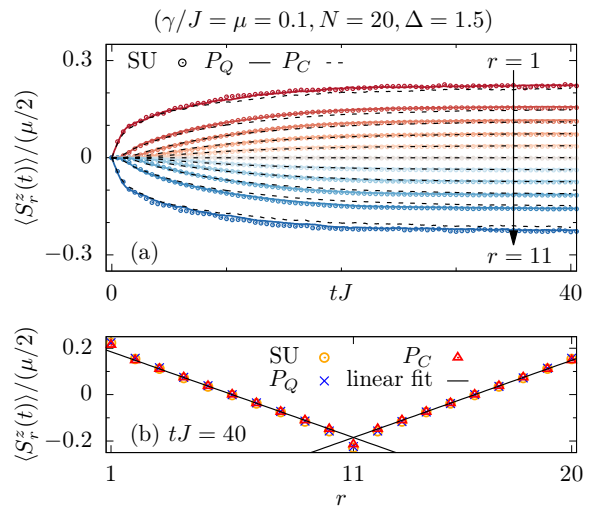


FIG. 2. Open-system dynamics for the model H' in Eq. (4), as obtained numerically for $\Delta = 1.5$, $\Delta' = 0$, $N = 20$, periodic boundary conditions, small coupling $\gamma/J = 0.1$, and weak driving $\mu = 0.1$. A simulation based on stochastic unraveling (SU) [72] is compared to two predictions, which are based on spatio-temporal correlation functions in the closed quantum system (P_Q) [72] and classical system (P_C). (a) Time evolution of the local magnetization $\langle S_r^z(t) \rangle$ for different sites r . (b) Site dependence of the steady state at $tJ = 40$.

IV. CLASSICAL LIMIT

To introduce the classical limit of our models, let us consider an arbitrary spin quantum number S . Then, the spin- S operators fulfill the usual commutation relations, which read

$$[S_r^i, S_{r'}^j] = i\hbar \delta_{rr'} \sum_k \epsilon_{ijk} S_r^k \quad (20)$$

with the Kronecker symbol $\delta_{rr'}$ and the antisymmetric Levi-Civita tensor ϵ_{ijk} . Here, we write \hbar explicitly, while it is otherwise set to unity. The classical counterpart of our models now results by taking the limit [78]

$$S \rightarrow \infty, \quad \hbar \rightarrow 0, \quad \hbar \sqrt{S(S+1)} = 1. \quad (21)$$

In this limit, the commutation relations in Eq. (20) turn into the Poisson-bracket relations

$$\{S_r^i, S_{r'}^j\} = \delta_{rr'} \sum_k \epsilon_{ijk} S_r^k \quad (22)$$

for real and three-dimensional spin vectors \mathbf{S}_r of unit length, $|\mathbf{S}_r| = 1$. The Hamilton operators H and H' in Eqs. (3) and (4) become Hamilton functions, but apart from that look the same. The total magnetization S^z is still strictly conserved, $\{H, S^z\} = \{H', S^z\} = 0$.

The Poisson-bracket relations in Eq. (22) also lead to Hamilton's equations of motion,

$$\frac{d}{dt} \mathbf{S}_r = \frac{\partial H}{\partial \mathbf{S}_r} \times \mathbf{S}_r, \quad (23)$$

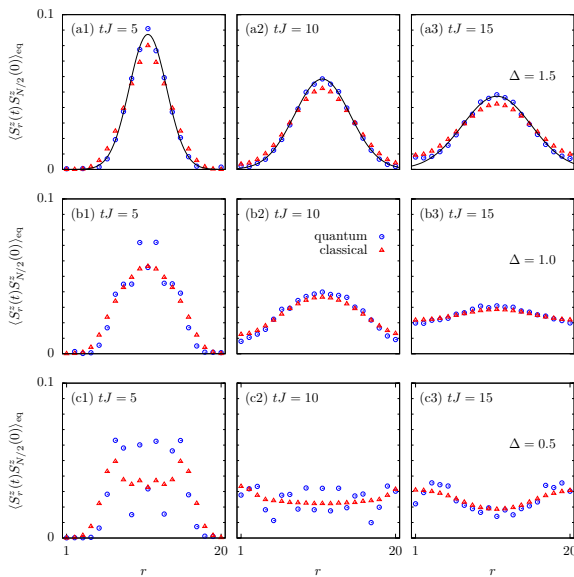


FIG. 3. Comparison of the site dependence of the quantum and classical correlation function $\langle S_r^z(t)S_{r'}^z(0) \rangle_{\text{eq}}$ for times $tJ = 5$ (first column), $tJ = 10$ (second column), and $tJ = 15$ (third column) for the model H' in Eq. (4) with $\Delta' = 0$, $N = 20$, and periodic boundary conditions. The anisotropy is $\Delta = 1.5$ (first row), $\Delta = 1.0$ (second row), and $\Delta = 0.5$ (third row). For $\Delta = 1.5$, Gaussian fits are indicated.

$$\frac{\partial H}{\partial \mathbf{S}_r} = \begin{pmatrix} S_{r-1}^x + S_{r+1}^x \\ S_{r-1}^y + S_{r+1}^y \\ \Delta(S_{r-1}^z + S_{r+1}^z) + \Delta'(S_{r-2}^z + S_{r+2}^z) \end{pmatrix}. \quad (24)$$

Physically, these equations describe the precession of a spin around a magnetic field, which is generated by the interaction with the neighboring spins. Mathematically, they are a coupled set of nonlinear differential equations, which is nonintegrable by means of the Liouville-Arnold theorem, even for $\Delta' = 0$ [79, 80], which is different to the quantum case $S = 1/2$. Therefore, for nontrivial initial conditions, they have to be solved numerically, as we also do here. Throughout our work, we employ a fourth-order Runge-Kutta scheme with a time step $\delta tJ = 0.01$, which is small enough to ensure that the total magnetization is well conserved during the time evolution.

Now, we come to the central objects in our work, i.e., the spatio-temporal correlation functions in the realm of classical mechanics. Focusing again on high temperatures $\beta = 1/T \rightarrow 0$, they read

$$\langle S_r^z(t)S_{r'}^z(0) \rangle_{\text{eq}} = \frac{1}{R_{\text{max}}} \sum_{R=1}^{R_{\text{max}}} S_r^z(t)S_{r'}^z(0), \quad (25)$$

where R_{max} is the number of realizations for different initial conditions, which are randomly drawn from a uniform distribution of points on a unit sphere. Formally, $R_{\text{max}} \rightarrow \infty$. In praxis, we average over as many realizations as $R_{\text{max}} = \mathcal{O}(10^8 - 10^9)$, to ensure that the remaining stochastic fluctuations are low. The need for

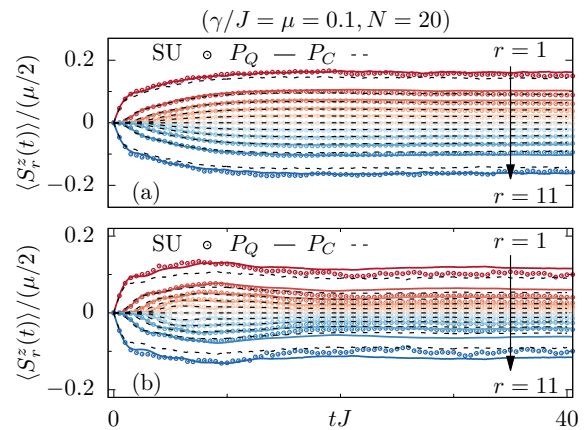


FIG. 4. Analogous data as the one in Fig. 2 (a), but now for (a) $\Delta = 1.0$ and (b) $\Delta = 0.5$. Quantum data are taken from Ref. [72].

such an extensive averaging in the numerical simulations is kind of compensated by the fact that the phase space grows only linearly with N , in contrast to the exponential growth of the Hilbert space. Due to this fact, we can particularly treat classical systems of quite large size N , which lie outside the possibilities of a quantum mechanical treatment. Still, we also consider small N to enable a comparison to quantum mechanics for the same size.

Eventually, coming back to the connection between the dynamics in open and closed systems, Eq. (15), the main idea is to replace the quantum correlation functions by the corresponding classical ones. When we do this strong simplification, the key question of our work is whether or not the time evolution in the open system can be still described accurately. To answer this question in a meaningful way, we first need to rescale the classical time by a factor

$$\tilde{S} = \sqrt{S(S+1)}, \quad (26)$$

which is $\tilde{S} \approx 0.87$ and close to one. Then, we additionally need to rescale the initial value of the classical correlation ($\langle S_r^z(0)S_{r'}^z(0) \rangle_{\text{eq}} = \delta_{rr'}/3$), since the one of the quantum correlation ($\langle S_r^z(0)S_{r'}^z(0) \rangle_{\text{eq}} = \delta_{rr'}/4$) is different. Apart from these rescalings, no further modifications are done and the dynamics as such is fully generated by Hamilton's equation of motion.

V. RESULTS

A. Nearest-neighbor interactions

Next, we turn to our numerical simulations, with the central aim to scrutinize to what degree the open-system quantum dynamics can be described by an approach on the basis of classical mechanics. Because we rely on the connection in Eq. (15), where correlation functions in the closed system are the main ingredient, we start with

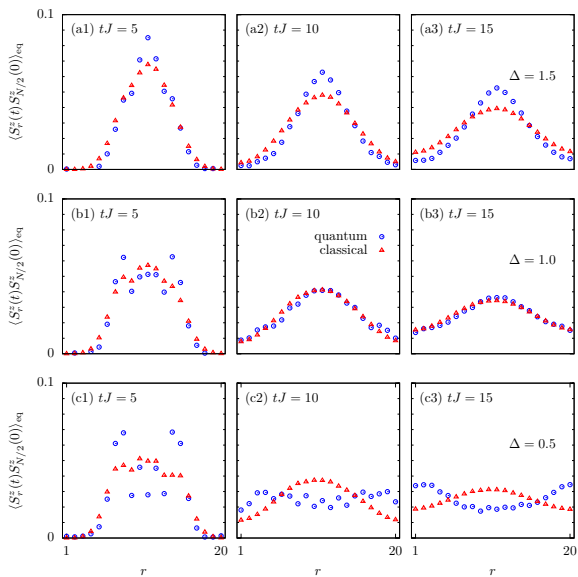


FIG. 5. The same data as the one in Fig. 3, but now with the next-to-nearest-neighbor interaction $\Delta' = 0.5$.

comparing quantum and classical correlation functions in the closed scenario. We do so for the spin-1/2 XXZ chain in Eq. (4) with $\Delta' = 0$ and $N = 20$. However, we also address the case of $\Delta' \neq 0$ and $N > 20$ later. The remaining parameters of the model are chosen to cover different quantum behaviors [21]: (a) diffusive behavior for $\Delta = 1.5$, (b) superdiffusive behavior for $\Delta = 1.0$, and (c) ballistic behavior for $\Delta = 0.5$. While our calculation of quantum correlations uses the concept of dynamical quantum typicality in its standard formulation [14, 15], our calculation of classical correlations is done in the way as outlined above. Similar comparisons can be found in the literature [65].

In Fig. 3, we summarize the comparison, by showing the site dependence of quantum and classical correlations for different times. As visible in Fig. 3 (first and second row), there is a quite convincing agreement for $\Delta = 1.5$ and 1.0. While minor deviations occur at short times, the overall site dependence is similar for longer times, which indicates that diffusion as such is not a prerequisite. Less convincing is the comparison for $\Delta = 0.5$. Still, quantum and classical correlations agree roughly and one might be tempted to conclude that the transport behavior is the same. However, the quantum case is well-known to be ballistic [21], while the classical case is likely diffusive, due to nonintegrability. Thus, the rough agreement reflects that the classical dynamics has still not reached the mean free path.

Using the correlations in Fig. 3, we now calculate the corresponding predictions for the time evolution of the open system, according to Eq. (15). In this calculation, we average over $T_{\max} = \mathcal{O}(10^4)$ different time sequences, which is enough to obtain sufficiently smooth curves. As already advertised before, Fig. 2 illustrates for $\Delta = 1.5$

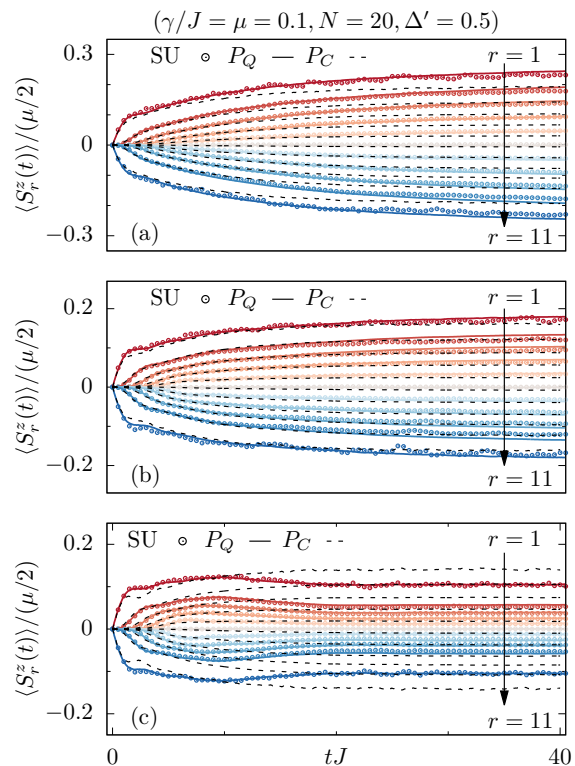


FIG. 6. The same data as the one in Figs. 2 (a) and 4, but now with the next-to-nearest-neighbor interaction $\Delta' = 0.5$. (a) $\Delta = 1.5$, (b) $\Delta = 1.0$, and (c) $\Delta = 0.5$. Quantum data are taken from Ref. [75].

a convincing agreement with existing simulations [72] on the basis of stochastic unraveling. In Fig. 4, we also depict a comparison for $\Delta = 1.0$ and 0.5. While the agreement for $\Delta = 1.0$ is also good, some disagreement is visible for $\Delta = 0.5$. Of course, one might expect this disagreement in view of the differences between quantum and classical correlations in Fig. 3 (third row). However, it should be noted that also the quantum prediction differs from the stochastic-unraveling data. This deviation can be traced back to the fact that the ballistic quantum motion for $\Delta = 0.5$ partially violates the equilibration assumption, which underlies the derivation of Eq. (15). In other words, while the injected excitation moves away from the boundary, it does not spread homogeneously over the system [72].

B. Next-to-nearest-neighbor interactions

Now, we allow for interactions between next-to-nearest sites and specifically choose a value of $\Delta' = 0.5$. Naively, one might expect that the overall agreement is improved, because the quantum and classical model become both nonintegrable for $\Delta' \neq 0$ and as a consequence should possess diffusion. However, this expectation turns out to be wrong.

In comparison to Fig. 3 for $\Delta' = 0$, the quantum and

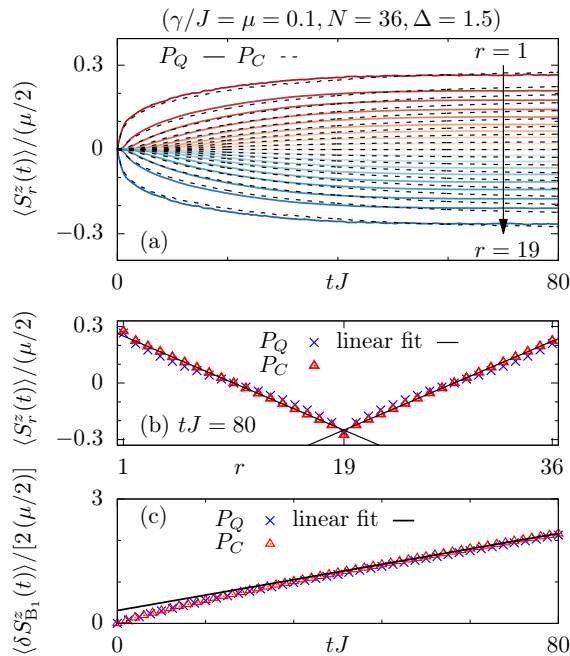


FIG. 7. (a) and (b) Similar data as the one in Fig. 2, but now for $N = 36$, where stochastic unraveling is not feasible any more. (c) Magnetization injected by the first bath as a function of time. Quantum data are taken from Ref. [72].

classical correlations in Fig. 5 for $\Delta' \neq 0$ do not agree as well as before. While the agreement for $\Delta = 1.0$ is again convincing, deviations start to set in for $\Delta = 1.5$. These deviations might be a signal that the quantum-classical correspondence eventually breaks down completely in the limit of very strong interactions. Yet, the correspondence is still satisfactory.

For $\Delta = \Delta' = 0.5$ in Fig. 5 (third row), the agreement turns out to be worst. While the quantum and classical case are both expected to exhibit diffusion, the quantum dynamics has not reached the mean free path, at least for the time scales considered. In contrast, the classical dynamics has reached the mean free path and already takes place in the hydrodynamic regime. Therefore, while transport might be qualitatively the same, it is quantitatively clearly different.

Using the correlations in Fig. 5, we again calculate the corresponding predictions for the time evolution of the open system. As can be seen, the quality of agreement in the closed system carries over to a similar quality in the open system. It is worth pointing out that the quantum prediction, in contrast to the classical prediction, is in excellent agreement with existing stochastic-unraveling data [75], for all values of Δ .

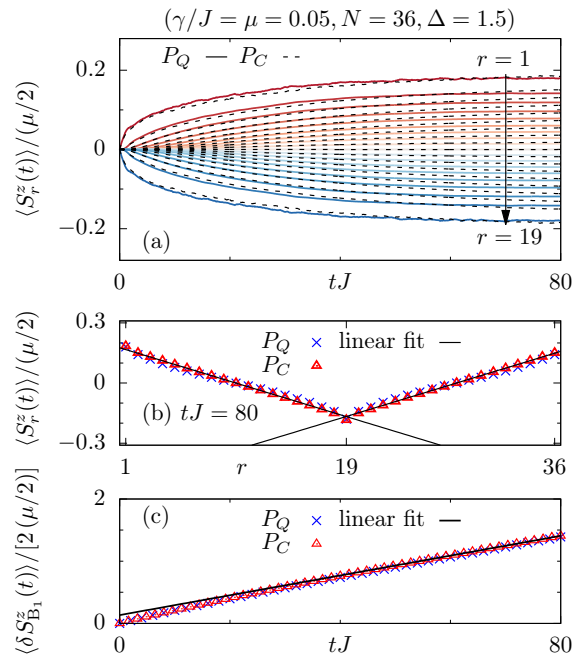


FIG. 8. Similar data as the one in Fig. 7, but now for different Lindblad parameters, i.e., for a smaller system-bath coupling $\gamma/J = 0.05$ and a weaker driving strength $\mu = 0.05$.

C. Larger system sizes

Next, we move forward to substantially larger system sizes. Here, stochastic unraveling is not feasible anymore and we cannot compare to corresponding data. Thus, we have to rely on a comparison between the quantum and classical predictions for the time evolution of the open system, as given in Eq. (15). We focus on the parameters $\Delta = 1.5$ and $\Delta' = 0$, which in our previous comparisons has turned out to be the best case. In Fig. 7, we depict results for $N = 36$, where the quantum prediction can still be carried out, due to existing data for correlations [72] from a calculation on a super computer. Apparently, the agreement between the two predictions for $N = 36$ is as convincing as for $N = 20$ considered before, which indicates that system size as such is not important for the accuracy of a classical treatment.

In Fig. 7 (c), we additionally depict a quantity, which we have not discussed so far. This quantity is the injected magnetization by the first bath,

$$\langle \delta S_{B_1}^z(t) \rangle \approx \frac{1}{T_{\max}} \sum_{T=1}^{T_{\max}} \delta d_{B_1, T}(t) \quad (27)$$

with

$$\delta d_{B_1, T}(t) = 2\mu \sum_j A_j \Theta(t - \tau_j) \langle [S_{B_1}^z(0)]^2 \rangle, \quad (28)$$

as discussed in the appendix in more detail. The injected magnetization is of interest, since from its time derivative, $d/dt \langle \delta S_{B_1}^z(t) \rangle$, the current in the steady state and

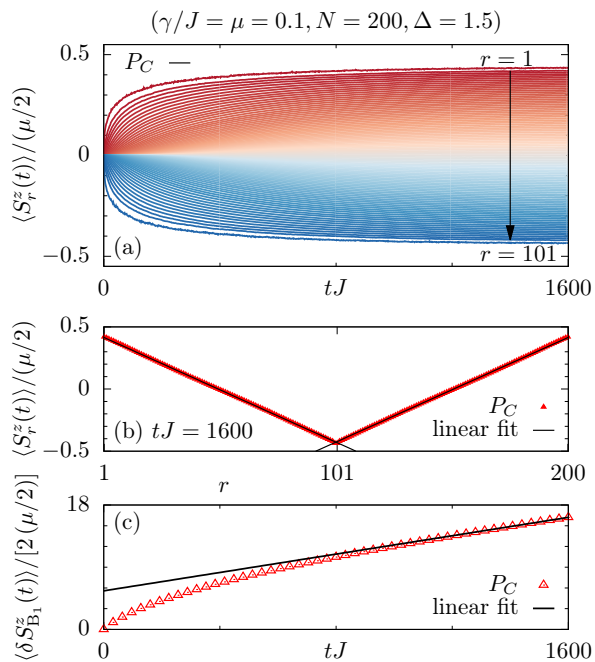


FIG. 9. Similar data as the one in Fig. 7, but now for a large system size $N = 200$. For this N , only classical mechanics is feasible. Note that the quality of the linear fit in (b) is much better for $N = 200$ (compared to $N = 36$), since the relative size of the bath-contact region is substantially smaller.

then a quantitative value for the diffusion constant can be calculated. As can be seen in Fig. 7 (c), the predictions for $\langle \delta S_{B_1}^z(t) \rangle$ are rather close to each other. Nevertheless, they still differ. Hence, we obtain two different diffusion coefficients,

$$D_Q/J \approx 0.99, \quad D_C/J \approx 0.84. \quad (29)$$

Because the prediction for the injected magnetization could be more sensitive to short-time deviations, as the ones visible in Fig. 3, we redo the analysis in Fig. 7 for $\gamma/J = 0.05$ (instead of $\gamma/J = 0.1$). In this way, the relevant time scale is increased. Simultaneously, we use another $\mu = 0.05$ (instead of $\mu = 0.1$) in Fig. 8. From this data, however, a significant change of the diffusion constants does not result,

$$D_Q/J \approx 1.01, \quad D_C/J \approx 0.86, \quad (30)$$

which indicates that we do not need to devote special attention to the role of the already small γ and μ , to extract quantitative values for transport constants.

It is instructive to compare the values for the diffusion constants in Eq. (30) to other values in the literature. In the classical case, a value of $D_C/J \sim 0.6$ has been found for the closed system [47], which is consistent with the value for the open system in Eq. (30). In the quantum case, the value is known with less precision and might be $D_Q/J \sim 0.6$ or larger in the closed system [21], while a value of $D_Q/J \approx 0.58$ has been found in the open system

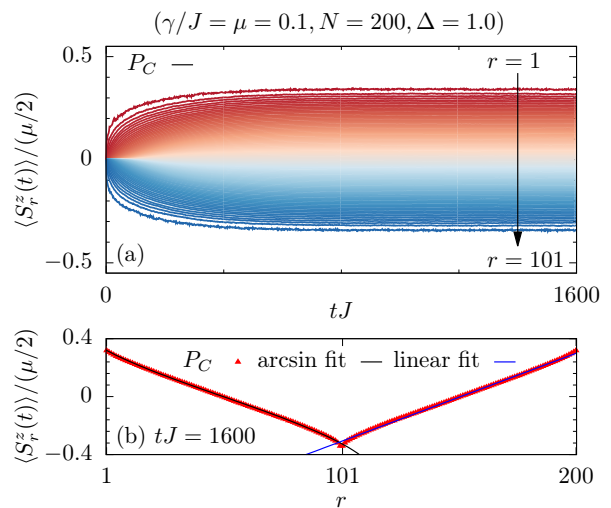


FIG. 10. Classical data for a large system size $N = 200$ and the isotropic point $\Delta = 1.0$. The other model parameters are the same as the ones in Fig. 9. For the steady-state profile in (b), a fit with the function $f(r) = a \arcsin[b(r - L/4)/(L/4)]$ is shown [24], in addition to a linear fit.

[23, 24], based on matrix-product-state simulations of the Lindblad equation, yet for a larger $\gamma/J = 1$.

Finally, we demonstrate in Fig. 9 explicitly that our classical approach can be used for as many as $N = 200$ lattice sites, where a quantum mechanical treatment is impossible, at least for the techniques used by us. While the required time to reach the steady state increases with N , the additional computing time poses no conceptual problem. This result is particularly relevant, since it is obtained for a small γ , which is hard to treat on the basis of matrix product states. For the diffusion constant, we find

$$D_C/J \approx 0.79, \quad (31)$$

which is close to $D_C/J \approx 0.84$ for $N = 36$, cf. Eq. (29), and indicates a good convergence w.r.t. system size.

Since Fig. 9 focuses on $\Delta = 1.5$, we depict in Fig. 10 additional $N = 200$ data for $\Delta = 1.0$. In comparison to $\Delta = 1.5$, the steady-state profile for $\Delta = 1.0$ is not as well described by a linear function. Thus, we perform in Fig. 10 (b) a fit with another function,

$$f(r) = a \arcsin \left[\frac{b(r - L/4)}{L/4} \right], \quad (32)$$

which has been used in the quantum case $S = 1/2$ before [24]. And indeed, also the classical case is well described by such a function, which indicates the usefulness of our classical approach for situations beyond the one of normal diffusion.

To further substantiate this claim and to conclude on the specific type of anomalous transport, we also depict in Fig. 11 classical data for the system-size dependence of the diffusion constant D . At the isotropic point $\Delta = 1.0$,

D increases with N and indicates superdiffusion [24]. In contrast, at $\Delta = 1.5$, D does not change significantly with N , as expected for diffusion. While we do not know the specific scaling function for $\Delta = 1.0$, we depict in Fig. 11 a power law and a logarithm as a guide to the eye. We should also stress that we cannot exclude a saturation in the large-system limit. For an early discussion of this topic, see Refs. [38, 39, 41, 42].

VI. CONCLUSION

In summary, we have studied the Lindblad equation, as a central approach to the physics of open quantum systems. In this context, we have particularly focused on boundary-driven transport, where a steady state emerges in the long-time limit, which features a constant current and a characteristic density profile. The starting point of our study has been a recently suggested connection [72] between the dynamics in open and closed systems, which exists in certain cases. We have built on this connection for magnetization transport in the spin-1/2 XXZ chain with and without next-to-nearest-neighbor interactions, as integrability breaking perturbations. Specifically, we have studied the question whether the time evolution of the open quantum system can be described by the use of classical correlation functions, as generated by the Hamiltonian equations of motion for classical real vectors. By comparing to exact numerical simulations of the Lindblad equation, we have found a good accuracy of such a description for a range of model parameters, but we have also pointed out counterexamples and its limitations for the quantitative extraction of transport coefficients. While this agreement is an interesting physical observation, it has also suggested that classical mechanics can be used to solve the Lindblad equation for comparatively large systems, which cannot be reached in a quantum mechanical treatment. Despite the approximate nature of this approach, one particular strength is the possibil-

ity to deal with small system-bath couplings, which are much harder to access on the basis of other numerical techniques.

An interesting question is the precise regime of validity of the quantum-classical correspondence of open systems within infinite-temperature spin-chain models. To answer it, one first has to know in which cases quantum and classical dynamics agree in the closed setup. Previous works like [64] suggest that such an agreement typically exists if the quantum model is nonintegrable, as it usually is for quasi-1D or 2D lattices. An agreement can also exist if the quantum model is integrable, as shown in Fig. 2. Yet, it necessarily requires that quasilocal conserved charges are of no relevance to the transport behavior [21], which is true for $\Delta > 1$ in Fig. 2, but not for $\Delta < 1$. An related point of view is that for $\Delta < 1$ the system is more XY-like and quantum correlations become important.

Another interesting question is the existence of a quantum-classical correspondence of open systems outside infinite temperature and spin models. Since our present work relies on the relation in and around Eq. (15), one first has to answer if this relation can be generalized to other models and finite temperatures, which is a promising direction of future research. Apart from the generalization of Eq. (15), it is clear that quantum and classical dynamics cannot agree for all models and finite temperatures, neither in the closed nor in the open setup. Already for spin systems, the nature of low-energy excitations can be different in the quantum and classical case. Moreover, some systems have no classical counterpart.

Acknowledgments

We thank Jochen Gemmer for fruitful discussions. This work has been funded by the Deutsche Forschungsgemeinschaft (DFG), under Grant No. 531128043, as well as under Grant No. 397107022, No. 397067869, and No. 397082825 within the DFG Research Unit FOR 2692, under Grant No. 355031190.

Appendix: Current in the steady state

In addition to the dynamics of the local magnetization, one can predict the current in the steady state. To this end, one needs the injected magnetization $\langle \delta S_{B_1}^z \rangle$ at the bath site B_1 , where the symbol δ is just a notation for the term “injected”. This injected magnetization can be predicted as [72]

$$\langle \delta S_{B_1}^z(t) \rangle \approx \frac{1}{T_{\max}} \sum_{T=1}^{T_{\max}} \delta d_{B_1, T}(t) \quad (\text{A.1})$$

with

$$\delta d_{B_1, T}(t) = 2\mu \sum_j A_j \Theta(t - \tau_j) \langle [S_{B_1}^z(0)]^2 \rangle, \quad (\text{A.2})$$

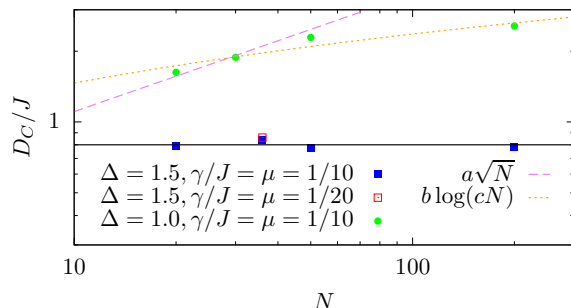


FIG. 11. Classical data for the system-size dependence of the diffusion constant D . While D does not change significantly with N for $\Delta = 1.5$, it increases with N for $\Delta = 1.0$, which indicates superdiffusion [24]. A power law and a logarithm are depicted as a guide to the eye.

which is slightly simpler than Eq. (15) in the main text and can be related to the current of interest. Since in the steady state all local currents are the same,

$$\langle j_r \rangle = \langle j_{r'} \rangle, \quad B_1 \leq r, r' \leq B_2, \quad (\text{A.3})$$

one only needs to know $\langle j_{B_1} \rangle$, which can be calculated as

$$\langle j_{B_1} \rangle = \frac{d}{dt} \frac{\langle \delta S_{B_1}^z(t) \rangle}{2}. \quad (\text{A.4})$$

Note that the factor 2 occurring in the denominator is due to periodic boundary conditions, as magnetization can flow to the right and left of the bath contact.

The diffusion constant follows from $\langle j_{B_1} \rangle$ via

$$D = -\frac{\langle j_{B_1} \rangle}{\langle S_{r+1}^z \rangle - \langle S_r^z \rangle} \quad (\text{A.5})$$

for some site r in the bulk of the system.

-
- [1] A. Polkovnikov, K. Sengupta, A. Silva, and M. Vengalattore, *Colloquium: Nonequilibrium dynamics of closed interacting quantum systems*, *Rev. Mod. Phys.* **83**, 863 (2011).
- [2] J. Eisert, M. Friesdorf, and C. Gogolin, *Quantum many-body systems out of equilibrium*, *Nat. Phys.* **11**, 124 (2015).
- [3] L. D'Alessio, Y. Kafri, A. Polkovnikov, and M. Rigol, *From quantum chaos and eigenstate thermalization to statistical mechanics and thermodynamics*, *Adv. Phys.* **65**, 239 (2016).
- [4] F. Borgonovi, F. Izrailev, L. Santos, and V. Zelevinsky, *Quantum chaos and thermalization in isolated systems of interacting particles*, *Phys. Rep.* **626**, 1 (2016).
- [5] D. A. Abanin, E. Altman, I. Bloch, and M. Serbyn, *Colloquium: Many-body localization, thermalization, and entanglement*, *Rev. Mod. Phys.* **91**, 021001 (2019).
- [6] I. Bloch, J. Dalibard, and W. Zwerger, *Many-body physics with ultracold gases*, *Rev. Mod. Phys.* **80**, 885 (2008).
- [7] J. Gemmer, M. Michel, and G. Mahler, *Quantum thermodynamics*, Lect. Notes Phys., Vol. 657 (Springer, Berlin, 2004).
- [8] S. Goldstein, J. L. Lebowitz, R. Tumulka, and N. Zanghì, *Canonical typicality*, *Phys. Rev. Lett.* **96**, 050403 (2006).
- [9] S. Popescu, A. J. Short, and A. Winter, *Entanglement and the foundations of statistical mechanics*, *Nat. Phys.* **2**, 754 (2006).
- [10] P. Reimann, *Typicality for generalized microcanonical ensembles*, *Phys. Rev. Lett.* **99**, 160404 (2007).
- [11] C. Bartsch and J. Gemmer, *Dynamical typicality of quantum expectation values*, *Phys. Rev. Lett.* **102**, 110403 (2009).
- [12] T. A. Elsayed and B. V. Fine, *Regression relation for pure quantum states and its implications for efficient computing*, *Phys. Rev. Lett.* **110**, 070404 (2013).
- [13] R. Steinigeweg, J. Gemmer, and W. Brenig, *Spin-current autocorrelations from single pure-state propagation*, *Phys. Rev. Lett.* **112**, 120601 (2014).
- [14] T. Heitmann, J. Richter, D. Schubert, and R. Steinigeweg, *Selected applications of typicality to real-time dynamics of quantum many-body systems*, *Z. Naturforsch. A* **75**, 421 (2020).
- [15] F. Jin, D. Willsch, M. Willsch, H. Lagemann, K. Michielsen, and H. De Raedt, *Random state technology*, *J. Phys. Soc. Jpn.* **90**, 012001 (2021).
- [16] J. M. Deutsch, *Quantum statistical mechanics in a closed system*, *Phys. Rev. A* **43**, 2046 (1991).
- [17] M. Srednicki, *Chaos and quantum thermalization*, *Phys. Rev. E* **50**, 888 (1994).
- [18] M. Rigol, V. Dunjko, and M. Olshanii, *Thermalization and its mechanism for generic isolated quantum systems*, *Nature* **452**, 854 (2008).
- [19] U. Schollwöck, *The density-matrix renormalization group*, *Rev. Mod. Phys.* **77**, 259 (2005).
- [20] U. Schollwöck, *The density-matrix renormalization group in the age of matrix product states*, *Ann. Phys.* **326**, 96 (2011).
- [21] B. Bertini, F. Heidrich-Meisner, C. Karrasch, T. Prosen, R. Steinigeweg, and M. Žnidarič, *Finite-temperature transport in one-dimensional quantum lattice models*, *Rev. Mod. Phys.* **93**, 025003 (2021).
- [22] M. Michel, M. Hartmann, J. Gemmer, and G. Mahler, *Fourier's Law confirmed for a class of small quantum systems*, *Eur. Phys. J. B* **34**, 325 (2003).
- [23] T. Prosen and M. Žnidarič, *Matrix product simulations of non-equilibrium steady states of quantum spin chains*, *J. Stat. Mech.* **2009**, P02035 (2009).
- [24] M. Žnidarič, *Spin transport in a one-dimensional anisotropic Heisenberg model*, *Phys. Rev. Lett.* **106**, 220601 (2011).
- [25] H.-P. Breuer and F. Petruccione, *The theory of open quantum systems* (Oxford University Press, 2007).
- [26] H. Wichterich, M. J. Henrich, H.-P. Breuer, J. Gemmer, and M. Michel, *Modeling heat transport through completely positive maps*, *Phys. Rev. E* **76**, 031115 (2007).
- [27] H. De Raedt, F. Jin, M. I. Katsnelson, and K. Michielsen, *Relaxation, thermalization, and Markovian dynamics of two spins coupled to a spin bath*, *Phys. Rev. E* **96**, 053306 (2017).
- [28] J. Dalibard, Y. Castin, and K. Mølmer, *Wave-function approach to dissipative processes in quantum optics*, *Phys. Rev. Lett.* **68**, 580 (1992).
- [29] M. Michel, O. Hess, H. Wichterich, and J. Gemmer, *Transport in open spin chains: A Monte Carlo wave-function approach*, *Phys. Rev. B* **77**, 104303 (2008).
- [30] M. Zwolak and G. Vidal, *Mixed-state dynamics in one-dimensional quantum lattice systems: A time-dependent superoperator renormalization algorithm*, *Phys. Rev. Lett.* **93**, 207205 (2004).
- [31] F. Verstraete, V. Murg, and J. I. Cirac, *Matrix product states, projected entangled pair states, and variational renormalization group methods for quantum spin systems*, *Adv. Phys.* **57**, 143 (2008).
- [32] H. Weimer, A. Kshetrimayum, and R. Orús, *Simulation methods for open quantum many-body systems*, *Rev. Mod. Phys.* **93**, 015008 (2021).
- [33] R. Kubo, M. Toda, and N. Hashizume, *Statistical physics*

- II: Nonequilibrium statistical mechanics*, Springer Series in Solid-State Sciences, Vol. 31 (Springer, Berlin, 1991).
- [34] C. G. Windsor, *Spin correlations in a classical Heisenberg paramagnet*, *Proc. Phys. Soc.* **91**, 353 (1967).
- [35] D. L. Huber, J. S. Semura, and C. G. Windsor, *Energy transport in magnetic chains*, *Phys. Rev.* **186**, 534 (1969).
- [36] N. A. Lurie, D. L. Huber, and M. Blume, *Computer studies of spin and energy transport in one-dimensional Heisenberg magnets*, *Phys. Rev. B* **9**, 2171 (1974).
- [37] H. De Raedt, J. Fizez, and B. De Raedt, *Energy fluctuations in a classical Heisenberg chain*, *Phys. Rev. B* **24**, 1562 (1981).
- [38] G. Müller, *Anomalous spin diffusion in classical Heisenberg magnets*, *Phys. Rev. Lett.* **60**, 2785 (1988).
- [39] R. W. Gerling and D. P. Landau, *Comment on “Anomalous spin diffusion in classical Heisenberg magnets”*, *Phys. Rev. Lett.* **63**, 812 (1989).
- [40] R. W. Gerling and D. P. Landau, *Time-dependent behavior of classical spin chains at infinite temperature*, *Phys. Rev. B* **42**, 8214 (1990).
- [41] O. F. de Alcantara Bonfim and G. Reiter, *Breakdown of hydrodynamics in the classical 1D Heisenberg model*, *Phys. Rev. Lett.* **69**, 367 (1992).
- [42] M. Böhm, R. W. Gerling, and H. Leschke, *Comment on “Breakdown of hydrodynamics in the classical 1D Heisenberg model”*, *Phys. Rev. Lett.* **70**, 248 (1993).
- [43] N. Srivastava, J.-M. Liu, V. S. Viswanath, and G. Müller, *Spin diffusion in classical Heisenberg magnets with uniform, alternating, and random exchange*, *J. Appl. Phys.* **75**, 6751 (1994).
- [44] V. Constantoudis and N. Theodorakopoulos, *Nonlinear dynamics of classical Heisenberg chains*, *Phys. Rev. E* **55**, 7612 (1997).
- [45] V. Oganessian, A. Pal, and D. A. Huse, *Energy transport in disordered classical spin chains*, *Phys. Rev. B* **80**, 115104 (2009).
- [46] D. Huber, *Spin diffusion in anisotropic Heisenberg chains: $S \geq 1/2$* , *Physica B* **407**, 4274 (2012).
- [47] R. Steinigeweg, *Spin transport in the XXZ model at high temperatures: Classical dynamics vs. quantum $s=1/2$ autocorrelations*, *EPL (Europhys. Lett.)* **97**, 67001 (2012).
- [48] A. S. de Wijn, B. Hess, and B. V. Fine, *Largest Lyapunov exponents for lattices of interacting classical spins*, *Phys. Rev. Lett.* **109**, 034101 (2012).
- [49] D. Bagchi, *Spin diffusion in the one-dimensional classical Heisenberg model*, *Phys. Rev. B* **87**, 075133 (2013).
- [50] T. Prosen and B. Žunkovič, *Macroscopic diffusive transport in a microscopically integrable Hamiltonian system*, *Phys. Rev. Lett.* **111**, 040602 (2013).
- [51] F. Jin, T. Neuhaus, K. Michielsen, S. Miyashita, M. A. Novotny, M. I. Katsnelson, and H. D. Raedt, *Equilibration and thermalization of classical systems*, *New J. Phys.* **15**, 033009 (2013).
- [52] B. Jencič and P. Prelovšek, *Spin and thermal conductivity in a classical disordered spin chain*, *Phys. Rev. B* **92**, 134305 (2015).
- [53] A. Das, S. Chakrabarty, A. Dhar, A. Kundu, D. A. Huse, R. Moessner, S. S. Ray, and S. Bhattacharjee, *Light-cone spreading of perturbations and the butterfly effect in a classical spin chain*, *Phys. Rev. Lett.* **121**, 024101 (2018).
- [54] A. Das, K. Damle, A. Dhar, D. A. Huse, M. Kulkarni, C. B. Mendl, and H. Spohn, *Nonlinear fluctuating hydrodynamics for the classical XXZ spin chain*, *J. Stat. Phys.* **180**, 238 (2019).
- [55] A. Das, M. Kulkarni, H. Spohn, and A. Dhar, *Kardar-Parisi-Zhang scaling for an integrable lattice Landau-Lifshitz spin chain*, *Phys. Rev. E* **100**, 042116 (2019).
- [56] N. Li, *Energy and spin diffusion in the one-dimensional classical Heisenberg spin chain at finite and infinite temperatures*, *Phys. Rev. E* **100**, 062104 (2019).
- [57] P. Glorioso, L. V. Delacrétaz, X. Chen, R. M. Nandkishore, and A. Lucas, *Hydrodynamics in lattice models with continuous non-Abelian symmetries*, *SciPost Phys.* **10**, 015 (2021).
- [58] A. J. McRoberts, T. Bilitewski, M. Haque, and R. Moessner, *Anomalous dynamics and equilibration in the classical Heisenberg chain*, *Phys. Rev. B* **105**, L100403 (2022).
- [59] D. Roy, A. Dhar, H. Spohn, and M. Kulkarni, *Robustness of Kardar-Parisi-Zhang scaling in a classical integrable spin chain with broken integrability*, *Phys. Rev. B* **107**, L100413 (2023).
- [60] L. Benet, F. Borgonovi, F. M. Izrailev, and L. F. Santos, *Quantum-classical correspondence of strongly chaotic many-body spin models*, *Phys. Rev. B* **107**, 155143 (2023).
- [61] A. J. McRoberts, T. Bilitewski, M. Haque, and R. Moessner, *Domain wall dynamics in classical spin chains: Free propagation, subdiffusive spreading, and soliton emission*, *Phys. Rev. Lett.* **132**, 057202 (2024).
- [62] T. A. Elsayed and B. V. Fine, *Effectiveness of classical spin simulations for describing NMR relaxation of quantum spins*, *Phys. Rev. B* **91**, 094424 (2015).
- [63] O. Gamayun, Y. Miao, and E. Ilievski, *Domain-wall dynamics in the Landau-Lifshitz magnet and the classical-quantum correspondence for spin transport*, *Phys. Rev. B* **99**, 140301 (2019).
- [64] D. Schubert, J. Richter, F. Jin, K. Michielsen, H. De Raedt, and R. Steinigeweg, *Quantum versus classical dynamics in spin models: Chains, ladders, and square lattices*, *Phys. Rev. B* **104**, 054415 (2021).
- [65] T. Heitmann, J. Richter, F. Jin, K. Michielsen, H. De Raedt, and R. Steinigeweg, *Spatiotemporal dynamics of classical and quantum density profiles in low-dimensional spin systems*, *Phys. Rev. Research* **4**, 043147 (2022).
- [66] P. Park, G. Sala, D. M. Pajerowski, A. F. May, J. A. Kolopus, D. Dahlbom, M. B. Stone, G. B. Halász, and A. D. Christianson, *Quantum and classical spin dynamics across temperature scales in the $S = 1/2$ Heisenberg antiferromagnet*, *arXiv:2405.08897* (2024).
- [67] R. Steinigeweg, M. Ogiewa, and J. Gemmer, *Equivalence of transport coefficients in bath-induced and dynamical scenarios*, *EPL (Europhys. Lett.)* **87**, 10002 (2009).
- [68] M. Žnidarič, *Nonequilibrium steady-state Kubo formula: Equality of transport coefficients*, *Phys. Rev. B* **99**, 035143 (2019).
- [69] A. Kundu, A. Dhar, and O. Narayan, *The Green-Kubo formula for heat conduction in open systems*, *J. Stat. Mech.* **2009**, L03001 (2009).
- [70] A. Purkayastha, S. Sanyal, A. Dhar, and M. Kulkarni, *Anomalous transport in the Aubry-André-Harper model in isolated and open systems*, *Phys. Rev. B* **97**, 174206 (2018).
- [71] A. Purkayastha, *Classifying transport behavior via current fluctuations in open quantum systems*, *J. Stat. Mech.*

- 2019**, 043101 (2019).
- [72] T. Heitmann, J. Richter, F. Jin, S. Nandy, Z. Lenarčič, J. Herbrych, K. Michielsen, H. De Raedt, J. Gemmer, and R. Steinigeweg, *Spin-1/2 XXZ chain coupled to two Lindblad baths: Constructing nonequilibrium steady states from equilibrium correlation functions*, *Phys. Rev. B* **108**, L201119 (2023).
- [73] C. R. Hogg, J. Glatthard, F. Cerisola, and J. Anders, *Stochastic simulation of dissipative quantum oscillators*, *arXiv:2406.05030* (2024).
- [74] The Lindblad description has a weak U(1) symmetry, which might be used to simplify exact diagonalization.
- [75] M. Kraft, J. Richter, F. Jin, S. Nandy, J. Herbrych, K. Michielsen, H. De Raedt, J. Gemmer, and R. Steinigeweg, *Lindblad dynamics from spatio-temporal correlation functions in nonintegrable spin-1/2 chains with different boundary conditions*, *Phys. Rev. Res.* **6**, 023251 (2024).
- [76] P. Fendley, *Strong zero modes and eigenstate phase transitions in the XYZ/interacting Majorana chain*, *J. Phys. A* **49**, 30LT01 (2016).
- [77] J. Kemp, N. Y. Yao, C. R. Laumann, and P. Fendley, *Long coherence times for edge spins*, *J. Stat. Mech.* **2017**, 063105 (2017).
- [78] In this work, we use only the limit in Eq. (21) and no additional semiclassical approximation.
- [79] V. I. Arnold, *Mathematical Methods of Classical Mechanics*, Graduate Texts in Mathematics (Springer, New York, 1978).
- [80] R. Steinigeweg and H.-J. Schmidt, *Heisenberg-integrable spin systems*, *Math. Phys. Anal. Geom.* **12**, 19 (2009).